

Supplemental information

**Microglial lipid phosphatase SHIP1 limits
complement-mediated synaptic pruning
in the healthy developing hippocampus**

Alessandro Matera, Anne-Claire Compagnion, Chiara Pedicone, M. Kotah Janssen, Andranik Ivanov, Katia Monsorno, Gwenaël Labouèbe, Loredana Leggio, Marta Pereira, Dieter Beule, Virginie Mansuy-Aubert, Tim L. Williams, Nunzio Iraci, Amanda Sierra, Samuele G. Marro, Alison M. Goate, Bart J.L. Eggen, William G. Kerr, and Rosa C. Paolicelli

Figure S1. Related to Figure 1

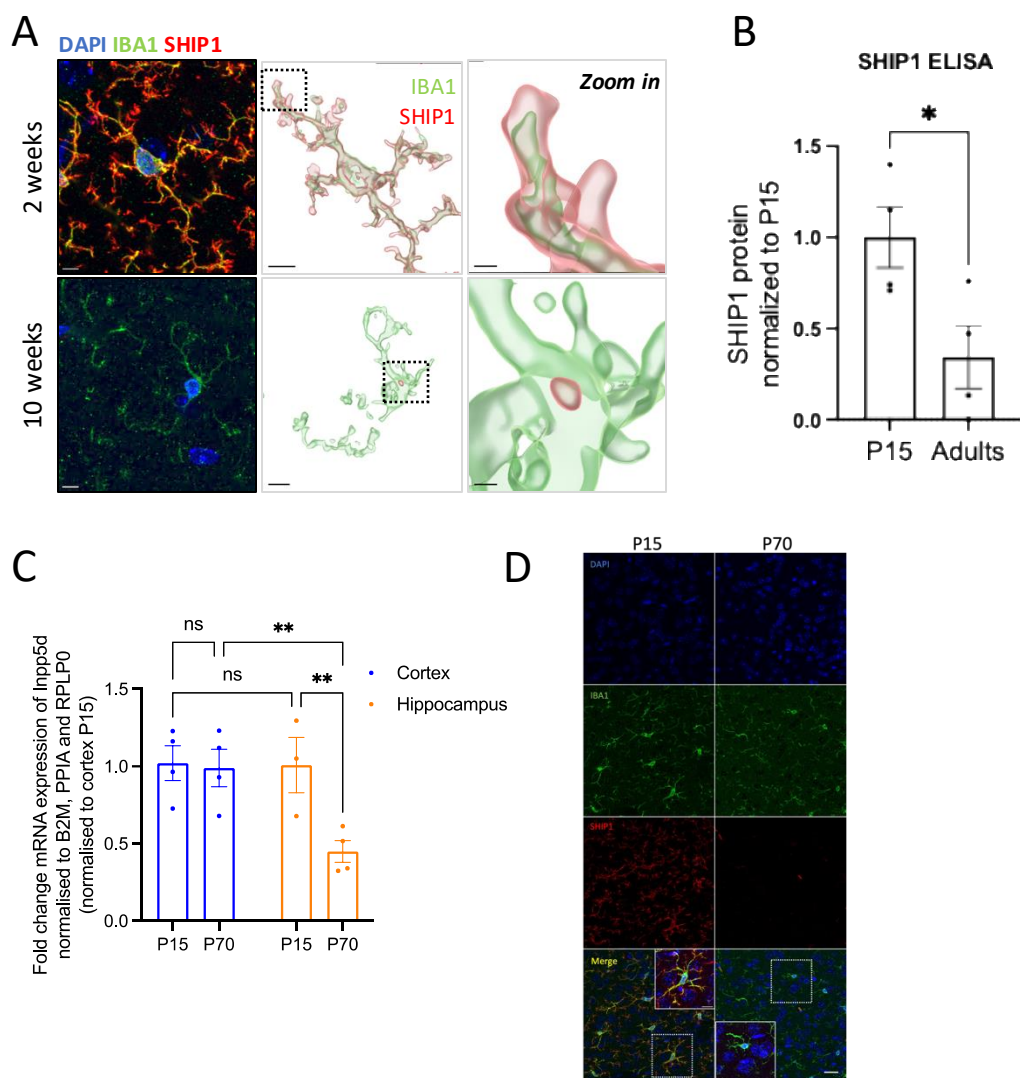


Figure S1. Inpp5d transcripts differ between hippocampus and cortical tissue

A) Representative confocal z-stack projections and relative 3D surface reconstruction of SHIP1 and IBA1 in microglia from the hippocampus of C57BL/6J WT mice, at 2 weeks and 10 weeks of age. Scalebar 5µm. Scalebar of Zoom in: 1µm. **B)** SHIP1 protein measured by ELISA immunoassay in cortical homogenates from P15 (N=4) and 12-14 weeks old (N=4) C57BL/6J WT mice. Unpaired t-test, *p<0.05. **C)** mRNA quantification by qRT-PCR of Inpp5d mRNA in isolated cortices and hippocampi from WT mice, collected at P15 and P70. Cortex at P15: N=4; cortex at P70: N=4; hippocampus at P15: N=3 and hippocampus at P70: N=4 mice. Two-way ANOVA, Tukey's multiple comparisons, **p<0.01 **D)** Representative z-stack confocal acquisitions of cortical layer II/III stained for IBA1, SHIP1 and DAPI, in C57BL/6J WT mice at P15 and P70. Scalebar 20µm. Scalebar zoom-in 5µm. Cells zoomed-in are highlighted in white.

Figure S2. Related to Figure 2

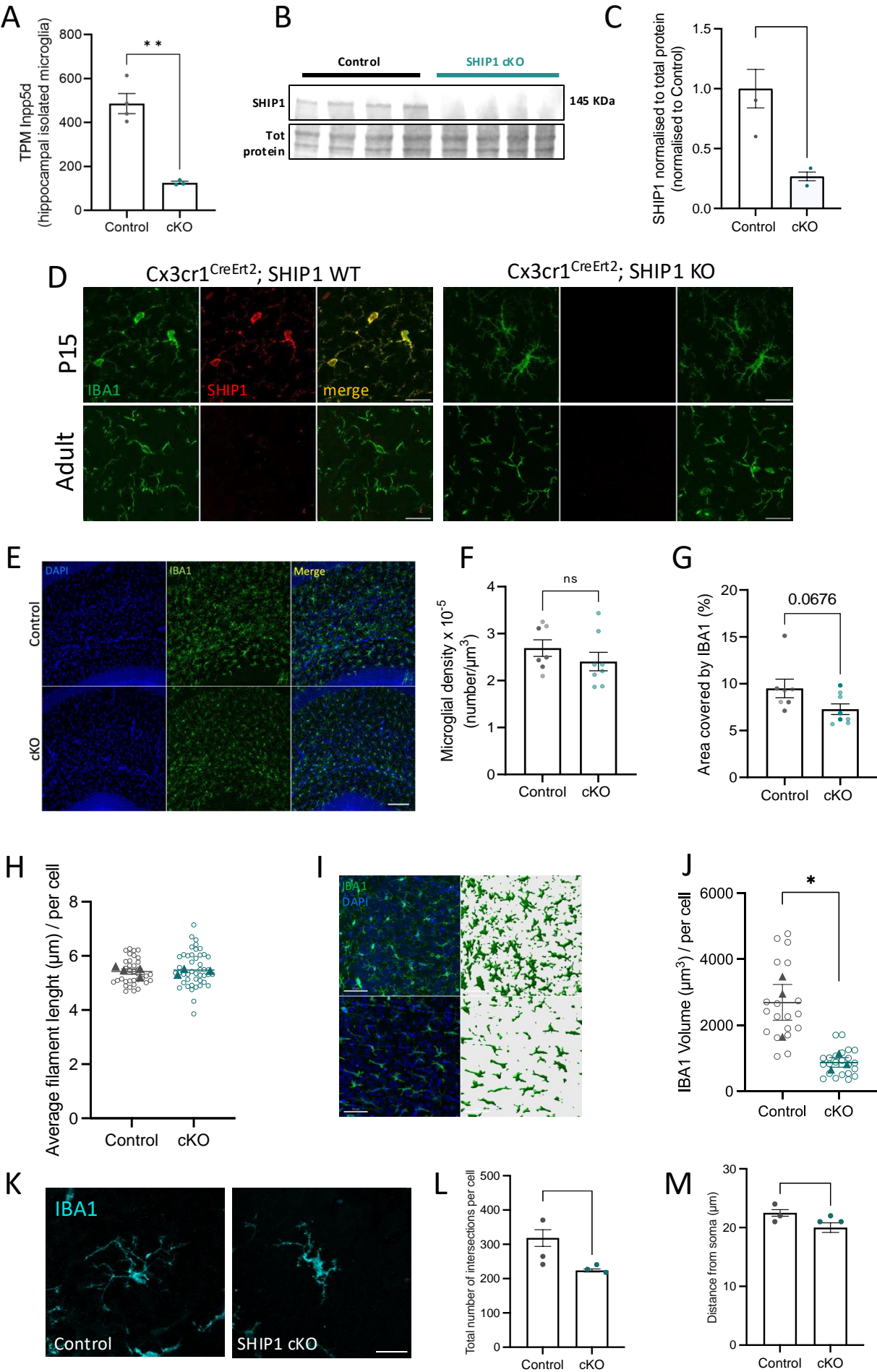


Figure S2. Microglial SHIP1 is reduced in cKO mice

A) Quantification of transcripts per millions (TPM) of *Inpp5d* assessed by bulk-RNA sequencing performed on FACS-isolated hippocampal microglia from control (N=4) and SHIP1 cKO (N=3) mice. Unpaired t-test, $^{**}p<0.01$. **B)** Western blot of SHIP1 and **C)** relative quantification, in the hippocampal homogenate of N=4 control and N=4 cKO mice. Unpaired t-test. $^{**}p<0.01$. **D)** Representative z-stack confocal projections in the hippocampal CA1 region of control and cKO mice at P15 and in adulthood (3 months old mice), immunostained for IBA1 and SHIP1. Scalebar: 30 μ m. **E)** Representative z-stack confocal projections of the CA1 hippocampus of control and cKO mice at P15, immunostained for IBA1. Scalebar 100 μ m. Quantification of **F)** microglia density and **G)** percentage of area covered by IBA1 signal. N=7 control vs N=8 SHIP1 cKO mice. **H)** Average filament length, quantified from n=36 control cells vs n=45 cKO cells, from N=7 control and N=8 SHIP1 cKO mice. Data refer to Figure 2D,E. **I)** Representative z-stack confocal projections and relative 3D reconstruction of the somatosensory cortex from control and cKO mice at P15. Scalebar 50 μ m. **J)** relative quantification of the IBA1 volume, Control: n=19 cells vs cKO: n=23 cells, from N=3 control and N=3 cKO mice. Unpaired t-test, $^{*}p<0.05$ **K)** Representative confocal z-stack projections of IBA1 positive microglia in the cerebellum; **L)** quantification of total number of intersections per cell, and **M)** distance from the soma, in control (N=6) and cKO (N=6) mice. Unpaired t-test. $^{*}p<0.05$, $^{**}p<0.01$. Females are shown in lighter and males in darker colors in all the graphs. Statistics are performed on animals.

Figure S3. Related to Figure 3

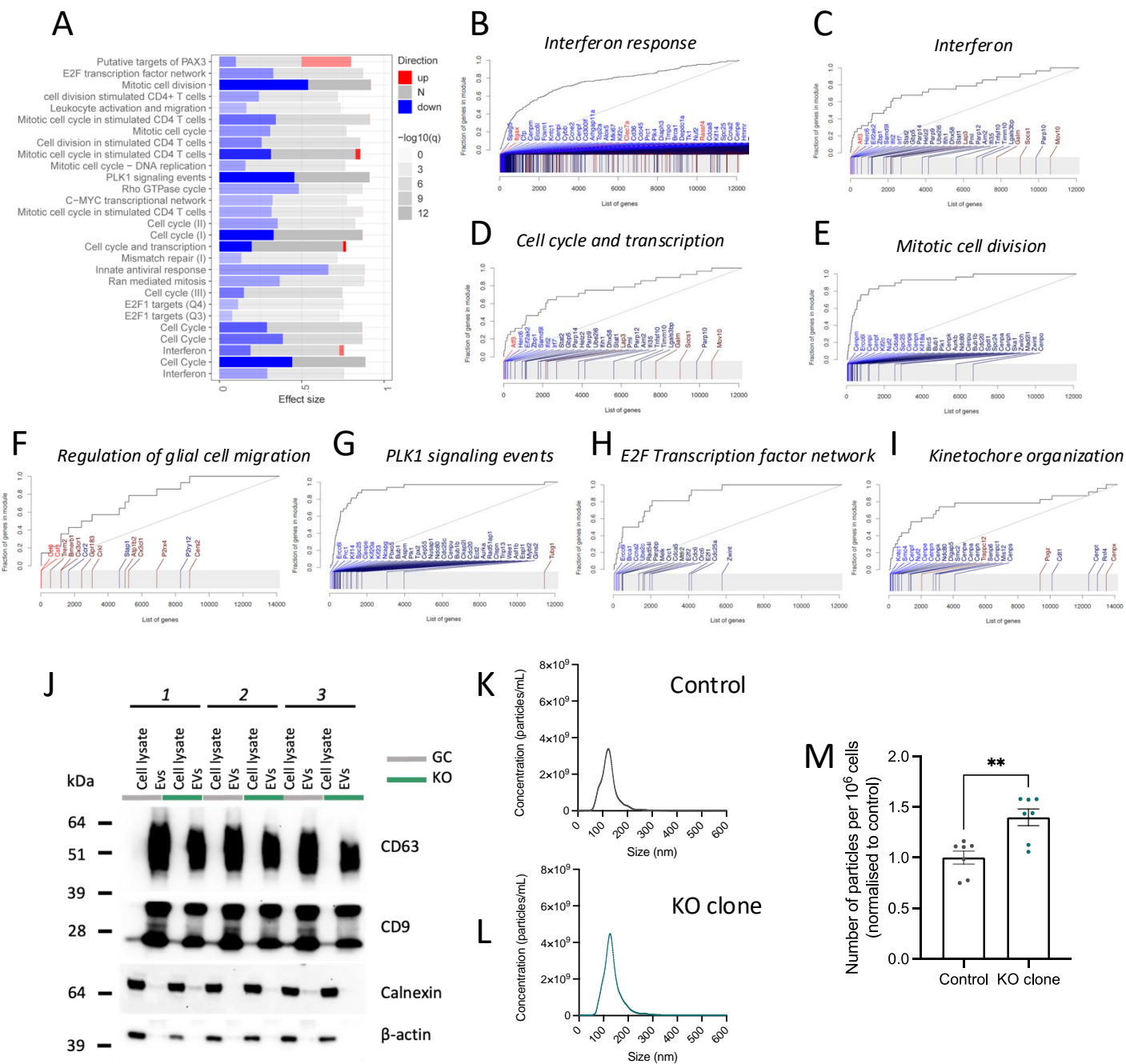


Figure S3. SHIP1 KO microglia show deregulation in cellular pathways and display increased release of extracellular vesicles

A) Msig-DB gene ontology molecular pathways significantly enriched in SHIP1 KO microglia. **B-I)** Evidence plots showing enriched gene sets in SHIP1 KO microglia (the name of the gene set is reported on top of the graph). X axis represents the full list of genes sorted by their p-values. Y axis is the cumulative fraction of genes from that gene set. Genes in blue are downregulated and red are upregulated in the SHIP1 KO. Light blue and light red correspond to significant deregulation (adj. P-value < 0.1). **J)** Representative western blot images for CD63, CD9, Calnexin and Actin in control and KO BV2 cell lysates and extracellular vesicles (EVs). Nanoparticle Tracking Analysis (NTA): Size distribution of EVs collected from **K)** control and **L)** SHIP1 KO BV2 culture media and **M)** relative quantification of the EV numbers normalized to control. Data are collected from 7 independent experiments. Unpaired t-test, **p<0.01.

Figure S4. Related to Figure 4

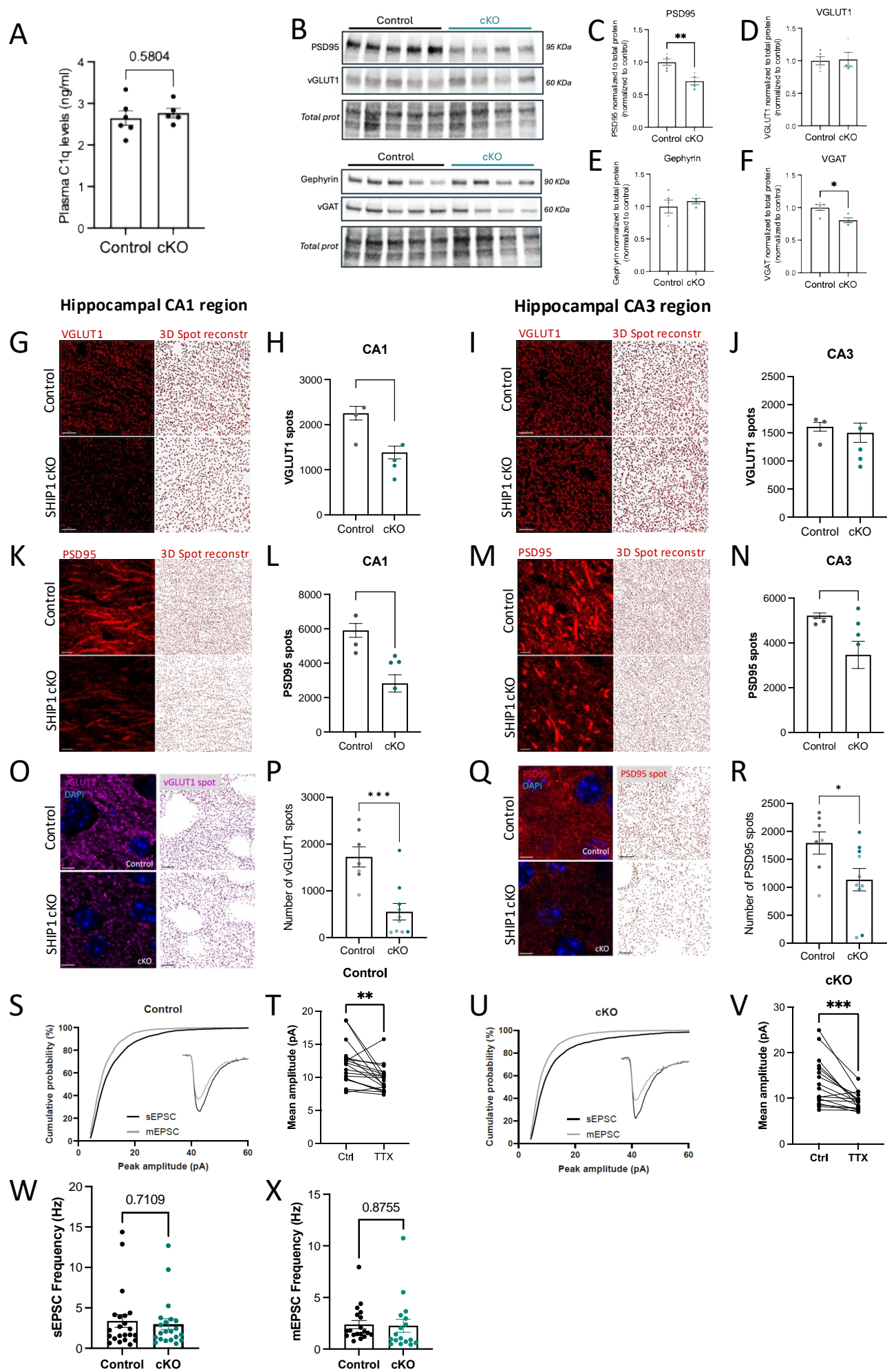


Figure S4. SHIP1 cKO mice at P15 display decreased synaptic density

A) C1q protein in the blood plasma from N=6 control and N=5 SHIP1 cKO mice at P15, measured by ELISA assay. Unpaired t-test $p=0.5804$. **B)** Western blot images of excitatory and inhibitory pre- and post-synaptic markers in the hippocampi of P15 control and SHIP1 cKO mice. Relative quantification of **C)** PSD95, **D)** VGLUT1, **E)** GEPHYRIN, **F)** VGAT protein expression, in N=5 control vs N=4 SHIP1 cKO mice. Unpaired t-test, $*p<0.05$, $**p<0.01$. Representative z-stack confocal projections and 3D spot reconstruction of VGLUT1 in **G)** hippocampal CA1 region and **I)** CA3 region, with relative quantification shown in **H)** and **J)**, respectively; scalebar: $7\mu\text{m}$. N=6 control vs N=7 cKO mice of both sexes (females represented in light and males in dark colors). Unpaired t-test, $**p<0.01$. Statistics are performed on animals. Representative z-stack confocal projections and 3D spot reconstruction of PSD95 in **K)** hippocampal CA1 region and **M)** CA3 region, with relative quantification shown in **L)** and **N)**, respectively; scalebar: $10\mu\text{m}$. N=6 control vs N=7 cKO mice of both sexes (females represented in light and males in dark colors). Unpaired t-test, $***p<0.001$, $*p<0.05$. Statistics are performed on animals. Representative z-stack projections and spot 3D reconstruction of confocal acquisitions of layer II-III cortices stained for **O)** VGLUT1 or **Q)** PSD95, with relative quantification shown in **P)** and **R)** respectively; scalebar $5\mu\text{m}$. N=7 control vs N=10 cKO mice of both sexes (females represented in light and males in dark colors). Unpaired t-test, $*p<0.05$, $***p<0.001$. **S)** Cumulative distribution of sEPSCs (no TTX, black line) and mEPSCs (TTX, gray line) amplitudes at P15 in neurons from control mice and **T)** relative quantification from control: $n=19-22$ cells, from N=5 mice. Paired t-test, $**p<0.01$. **U)** Cumulative distribution of sEPSCs (no TTX, black line) and mEPSCs (TTX, gray line) amplitudes at P15 in neurons from cKO mice and **V)** relative quantification from cKO: $n=17-21$ cells, from N=5 mice. Paired t-test, $***p<0.001$. Mean frequency of **W)** sEPSC and **X)** mEPSC from control and cKO mice. Unpaired t-test, $p>0.05$, ns.

Figure S5. Related to Figure 5

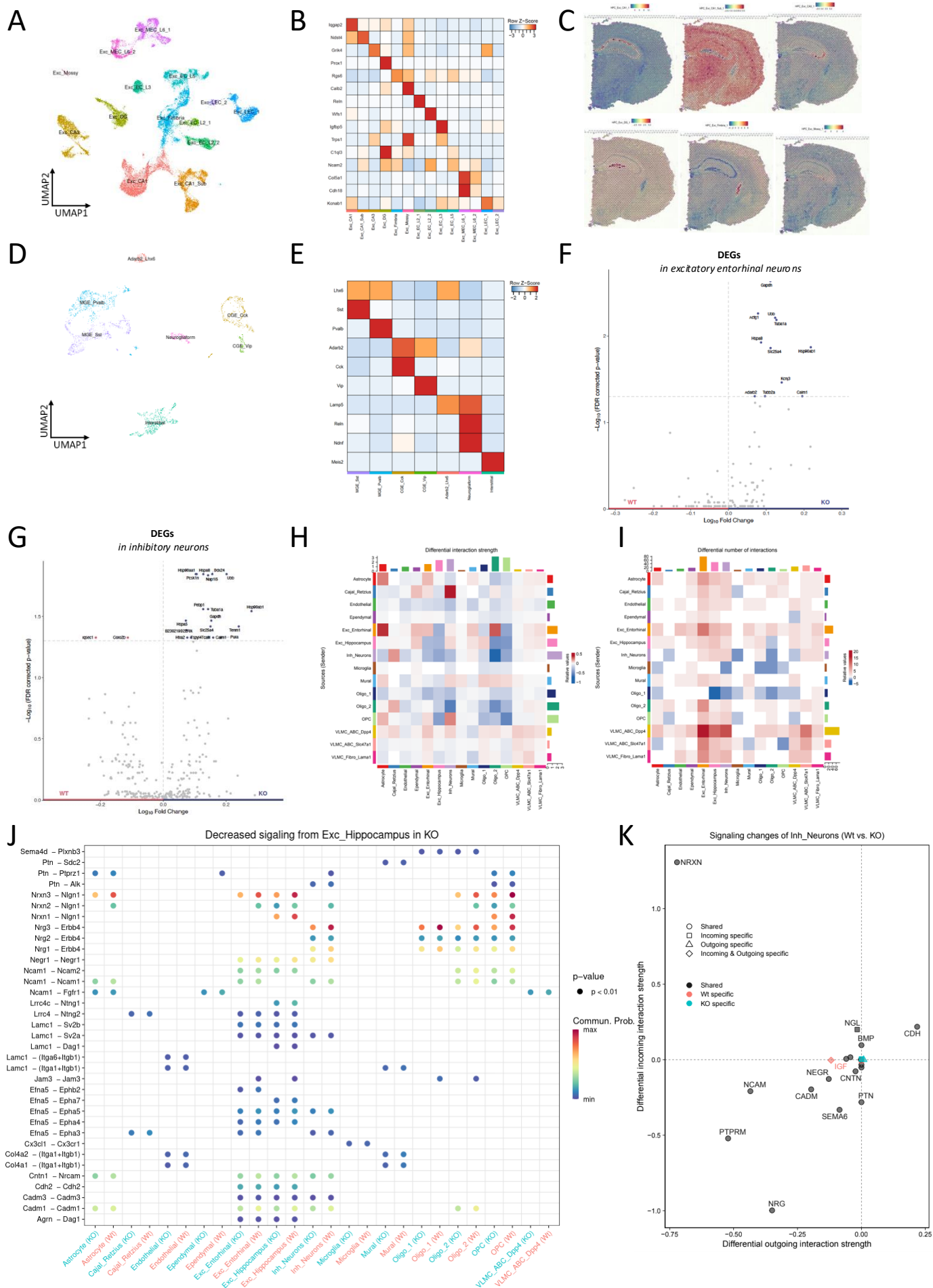
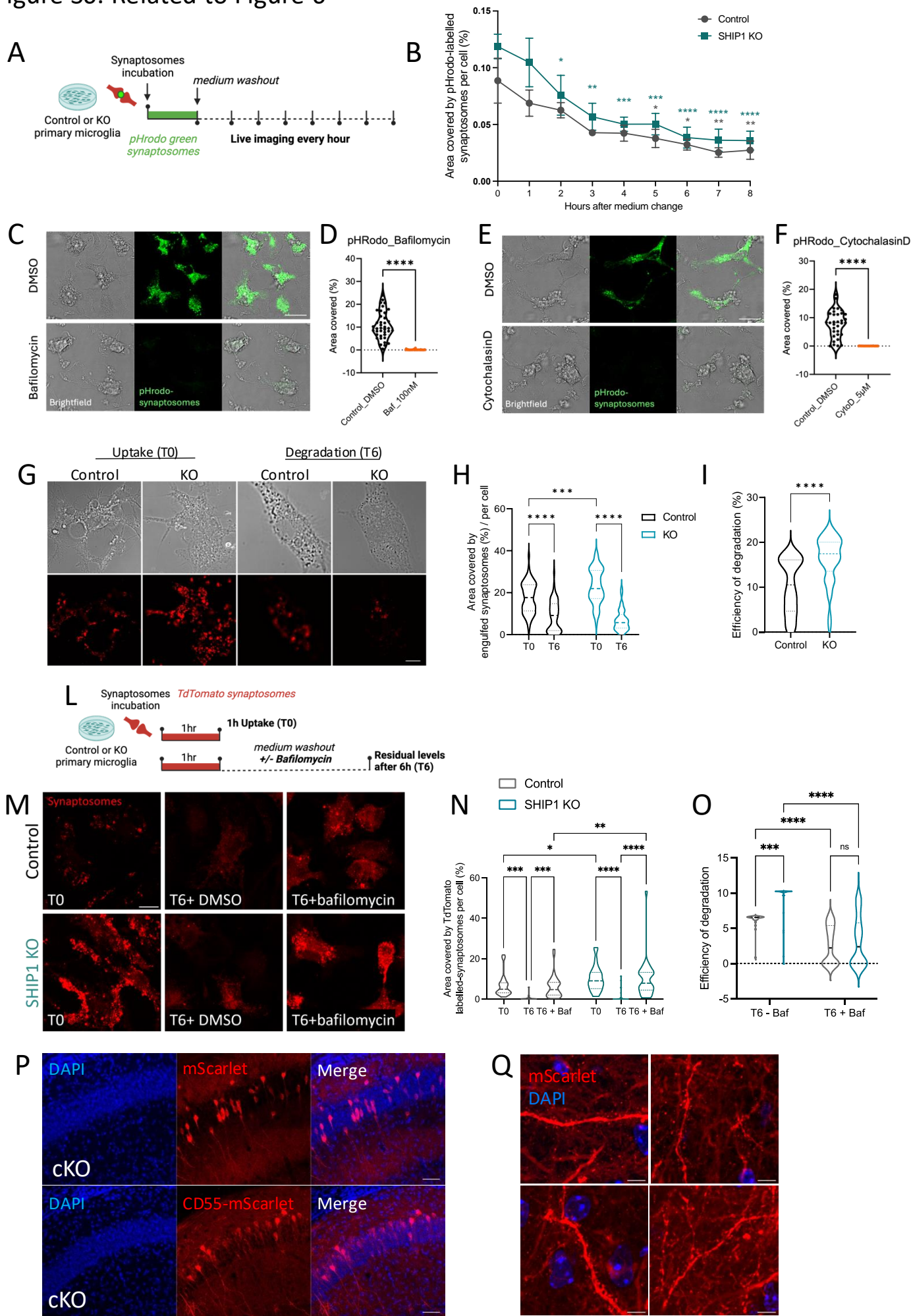


Figure S5. snRNAseq predicts defective inhibitory and excitatory neuronal connections

A) Sub-clustering of 31961 excitatory neurons, represented on a UMAP. **B)** Heatmap of representative cluster markers, including known entorhinal cortex layer markers. **C)** Confirmation and spatial localization of hippocampal neuronal clusters by plotting the top 100 cluster markers as module scores on a publicly available Visium dataset from 10x Genomics. **D)** Sub-clustering of 3446 inhibitory neurons, represented on a UMAP. **E)** Heatmap of representative cluster markers. **F)** Volcano plot of differentially expressed genes in aggregated excitatory entorhinal neurons (A) and **G)** volcano plot of differentially expressed genes in aggregated inhibitory neurons (D) based on MAST analysis, using FDR adjusted p-value < 0.05 as a threshold. Heatmap depicting the **H)** net interaction strength and **I)** net number of interactions predicted by CellChat re-analysis after collapsing neuronal cell types into excitatory hippocampal, excitatory-entorhinal, and inhibitory. Blue color indicates a relative decrease in cKO, while red indicates a relative increase in cKO. **J)** Overview of signaling pathways from excitatory hippocampal neurons that are relatively decreased in the cKO group, with predicted targets shown on the x-axis. **K)** Net signaling changes in interneurons as predicted by CellChat, with positive values corresponding to enrichment in cKO, and negative values corresponding to enrichment in WT. X-axis depicts pathways for which the corresponding interneurons are the source, while y-axis depicts pathways for which interneurons are targets.

Figure S6. Related to Figure 6



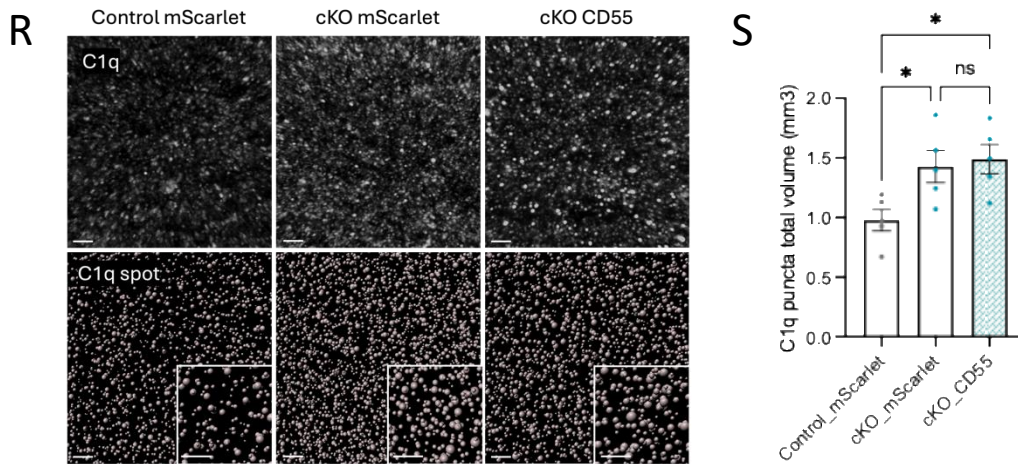
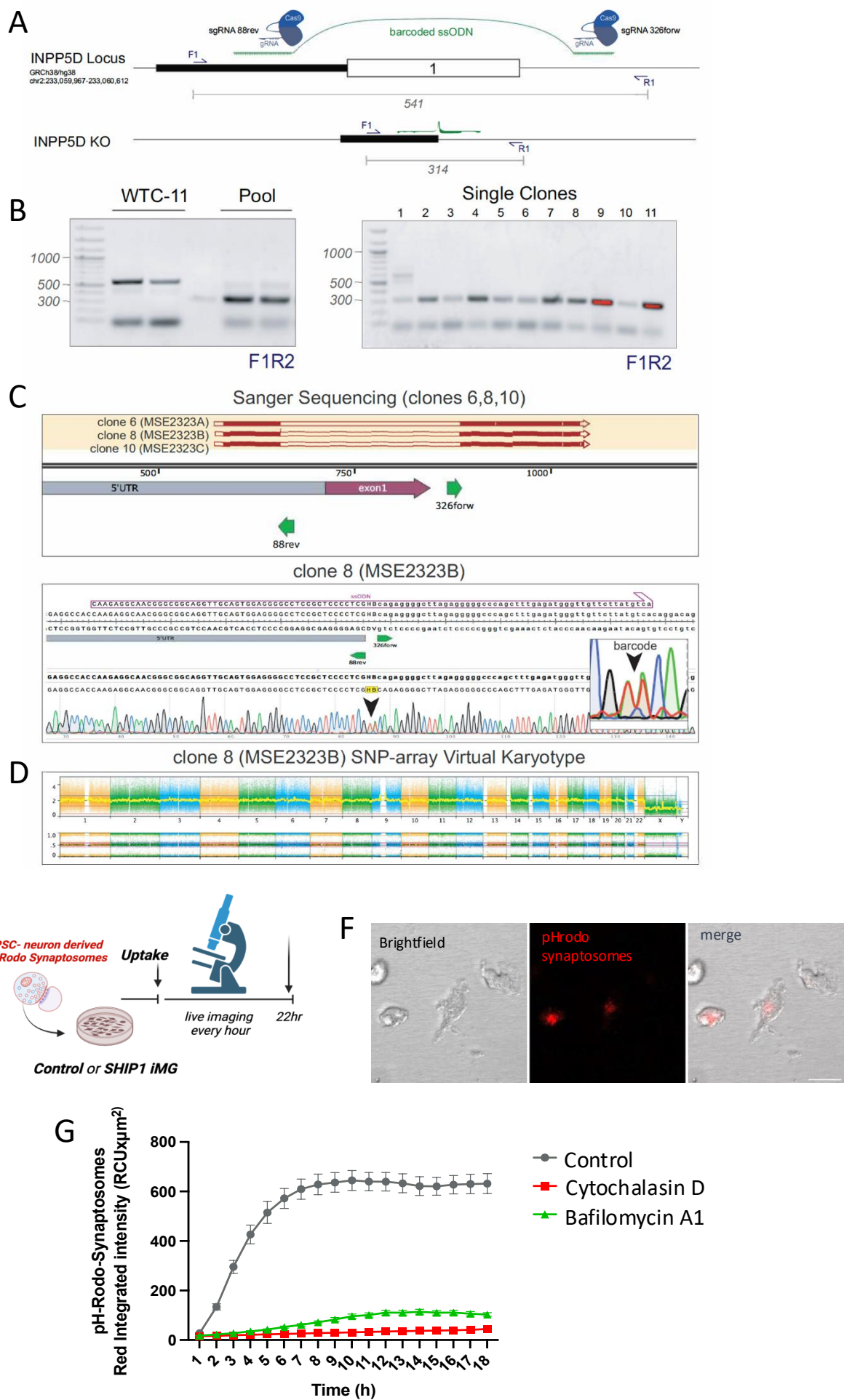


Figure S6. SHIP1 KO in microglia display enhanced synaptosome phagocytosis *in vitro* and depends on the complement system *in vivo*

A) Experimental paradigm for live imaging of synaptosome engulfment assay using 488-pHrodo-labelled synaptosomes. **B)** Relative quantification of the area covered by 488-pHrodo-labelled synaptosome measured by confocal imaging over time, after medium washout. Two-way repeated measures ANOVA, Dunnett's multiple comparison test for each time point against its own initial T0. * $p<0.05$, ** $p<0.01$, *** $p<0.001$, **** $p<0.0001$. **C)** Representative z-stack confocal acquisitions of 488-pHrodo-labelled synaptosome engulfed by control primary microglia with or without bafilomycin A1 and **D)** relative quantification of the area covered by the pHrodo signal per cell. Scalebar: 20 μ m. N=39 control and N=37 KO cells. Unpaired t-test, **** $p<0.0001$. **E)** Representative z-stack confocal acquisitions of 488-pHrodo-labelled synaptosome engulfed by control primary microglia with or without cytochalasin D, and **F)** relative quantification of the area covered by the pHrodo signal per cell. Scalebar: 20 μ m. N=33 control and N=25 KO cells. **G)** Representative z-stack confocal acquisitions of primary SHIP1 KO and control microglia, incubated with TdTomato-labelled synaptosomes: uptake (T0) and degradation (T6); scalebar 10 μ m. **H)** Relative quantification of area covered by the cargo per cell and **I)** efficiency of degradation. In **(H)**: Two-way ANOVA, Tukey's multiple comparison test: *** $p<0.001$, **** $p<0.0001$. In **(I)**: Unpaired t-test, **** $p<0.0001$. T0: control n=64 cell, KO n=56 cells. T6: control n=56 cells, KO n=37 cells. Data are averaged from N=3 independent experiments, using N=3 control and N=3 KO independent primary microglia isolations. **L)** Experimental paradigm for synaptosome engulfment assay using TdTomato-labelled synaptosomes in presence or absence of bafilomycin A1. **M)** Representative z-stack confocal acquisitions of primary SHIP1 KO and control microglia, incubated with TdTomato-labelled synaptosomes: uptake (T0), degradation (T6) and following Bafilomycin incubation for 6 hours (T6+Bafilomycin); scalebar 10 μ m. **N)** Relative quantification of **M)** showing the area covered by the TdTomato signal per cell. In **O)** the efficiency of degradation is shown per control and KO cells, in presence or absence of Bafilomycin. Two-way ANOVA, Šídák's multiple comparisons test: * $p<0.05$, ** $p<0.01$, *** $p<0.001$, **** $p<0.0001$. Control: T0, n=30; T6 n=26; T6+Baf n=33. SHIP1 KO: T0, n=26; T6 n=33; T6+Baf n=28 cells. **P)** Representative z-stack confocal acquisitions of SHIP1 cKO CA1 hippocampi, injected with either AAV-mScarlet or AAV-CD55-P2A virus at P0-P1. Images are acquired at P15. Scalebar 50 μ m. **Q)** Representative z-stack confocal acquisitions on the hippocampal CA1 region from animals injected with AAV-mScarlet, showing mScarlet expression in dendrites and dendritic spines at P15. Scale bar 5 μ m. **R)** Representative z-stack confocal images and relative 3D spot reconstruction of C1q puncta in the hippocampal CA1 at P15 from control mice injected with AAV-mScarlet, and from cKO mice injected with AAV-mScarlet or AAV-CD55-P2A-mScarlet virus. **S)** Quantification of the total C1q+ volume in **R)** N=5 control mScarlet, N=5 SHIP1 cKO mScarlet, N=5 SHIP1 cKO CD55-mScarlet. One-way ANOVA, Tukey's multiple comparisons test, * $p<0.05$. Multiple sections have been analyzed over independent experiments. Statistics are performed on animals.

Figure S7. Related to Figure 7



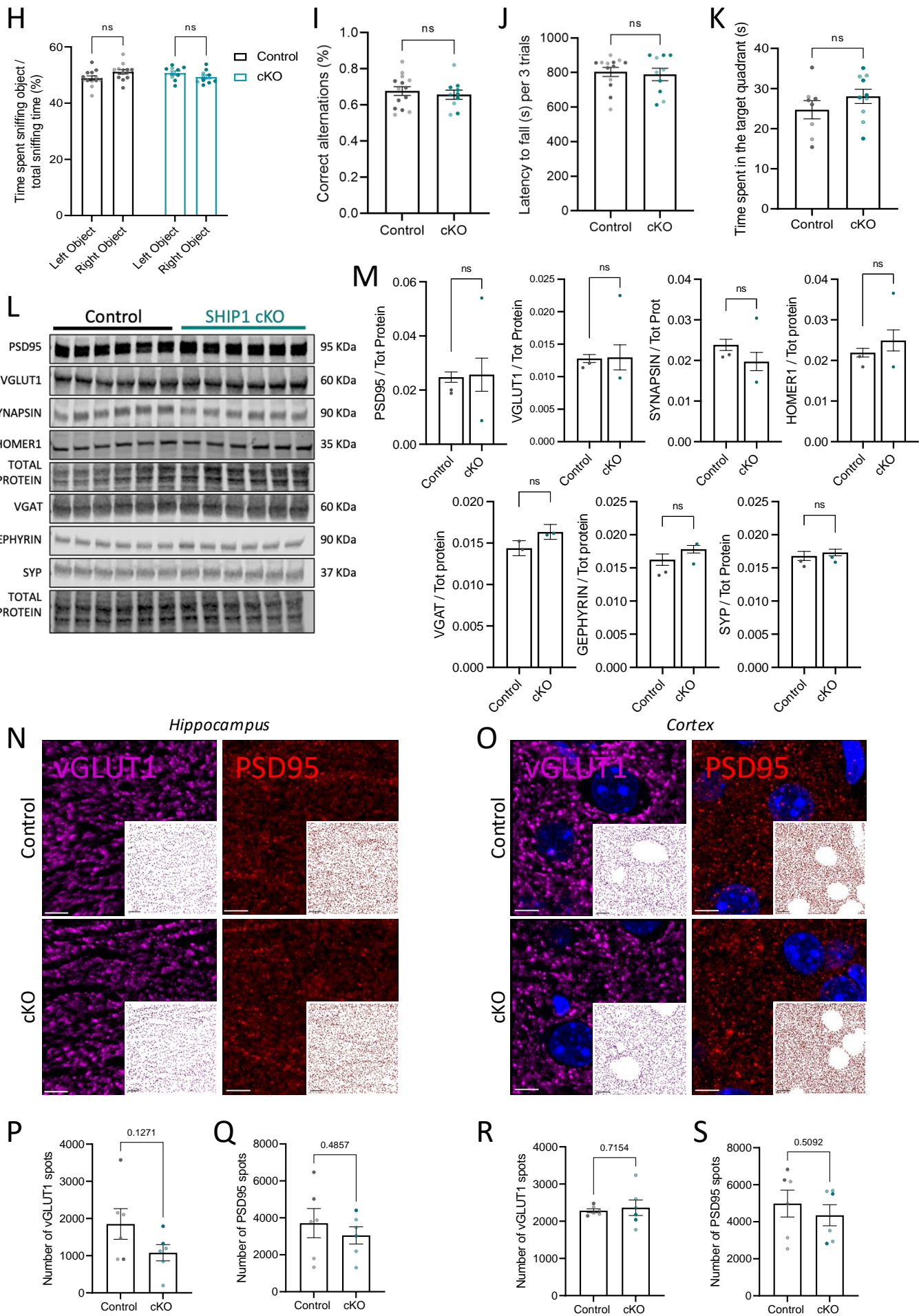


Figure S7. Validation of SHIP1 KO iMG

A) Schematic of the CRISPR/Cas9-mediated genome editing strategy used to generate homozygous SHIP1 knockout human iPSC lines (see Methods). Two sgRNAs were employed: one targeting the 5'UTR (88rev) and another targeting intron 1 (326forw). These were used in combination with a barcoded, bridging ssODN to facilitate exon 1 excision via homology-directed repair (HDR). The barcode in the ssODN—two degenerate nucleotides between the homology arms, differing from adjacent genomic bases (in this case, represented by H and B)—aided in screening for homozygous clones via detection of a double peak in Sanger sequencing. **B)** PCR screening with primers F1 and R2 was performed to detect the 227 bp deletion (shift from 541 bp to 314 bp), confirming the deletion in the iPSC pool post-nucleofection with CRISPR/Cas9 reagents and in 11 single clones, but not in the parental iPSC line (WTC11). **C)** Sanger sequencing of the F1-R1 PCR product confirmed the 227 bp deletion in single clones 6, 8, and 10 and revealed the double-peak barcode in clone 8 (MSE2323B), confirming the homozygosity of the HDR. **D)** A virtual karyotype via SNP-array confirmed the normal karyotype of MSE2323B. No CNVs or AOH larger than 1.5 Mb were detected on somatic chromosomes using SNP-array. The typical WTC-11 deletion of 2.9 Mb at Yp11.2, known to be present in the donor from whom the cell line was derived, was detected. **E)** Experimental paradigm of synaptosome engulfment by iMG with hiPSC-neuron derived pHrodo-red-labelled synaptosomes. **F)** Representative confocal acquisition of iMG showing internalized phrodo-labelled synaptosomal cargo. **G)** Quantification of integrated intensity object average ($\times \mu\text{m}^2$) over time for control iMG, and iMG treated either with cytochalasin D or bafilomycin A1, showing that the pHrodo signal is abolished when phagocytosis or lysosomal acidification are inhibited, respectively. Data are the average of N=6 measures per condition in one biological experiment.

Adult mice injected with tamoxifen at P3-P4: **H)** Novel object recognition test in. Percentage of the time spent exploring objects (familiar and novel object). N=13 control vs N=10 SHIP1 cKO mice. **I)** Y-maze test. Percentage of correct alternations counted during the test. N=13 control vs N=10 SHIP1 cKO mice. **J)** Rotarod test. Cumulative latency to fall from the rod, shown as the sum of three trials. N=13 control vs N=10 SHIP1 cKO mice. Females are indicated in light and males in dark colors. **K)** Time spent in the target quadrant during the test phase of the Barnes maze. **L)** Western blot images of excitatory and inhibitory pre- and post-synaptic markers in the hippocampi of adult control and SHIP1 cKO mice and **M)** relative quantification of PSD95, VGLUT1, SYNAPSIN, HOMER1, VGAT, GEPHYRIN and SYNAPTOPHYSIN protein normalized to total protein expression. N=6 control vs N=6 SHIP1 cKO mice. Unpaired t-test. **N,O)** Representative z-stack confocal projections of adult hippocampi and layer II-III cortices stained for DAPI, vGLUT1 or PSD95, along with their relative spot 3D reconstruction. Relative quantification of VGLUT1 and PSD95 number of spots in **P,Q)** the hippocampus and **R,S)** the cortex. Scalebar 5 μm . N=6 control vs N=6 cKO mice of both sexes (females represented in light and males in dark colors). Unpaired t-test.